FEBS Letters 580 (2006) 2033–2040

Putative aggregation initiation sites in prion protein

Jan Ziegler[a,1], Christine Viehrig[a,1], Stefan Geimer[b], Paul Rösch[a], Stephan Schwarzinger[a,*]

[a] *Lehrstuhl Biopolymere, University Bayreuth, Universitaetsstrasse 30, 95447 Bayreuth, Germany*
[b] *Department of Biology/Electron Microscopy, University Bayreuth, Universitaetsstrasse 30, 95447 Bayreuth, Germany*

Received 16 December 2005; revised 22 February 2006; accepted 1 March 2006

Available online 10 March 2006

Edited by Jesus Avila

Abstract Misfolded prion protein, PrP^{Sc}, is believed to be the pathogenic agens in transmissible spongiform encephalopathies. Little is known about the autocatalytic misfolding process. Looking at the intrinsic properties of short sequence stretches, such as conformational flexibility and the tendency to populate extended conformers, we have examined the aggregation behaviour of various peptides within the region 106–157 of the sequence of human prion protein. We observed fast aggregation for the peptide containing residues I138-I-H-F141. This sequence, which is presented at the surface of cellular prion protein, PrP^{C}, in an almost β-sheet-like conformation, is therefore an ideal anchor-point for initial intermolecular contacts leading to oligomerization. We further report that the aggregation propensity of the neurotoxic peptide 106–126 appears to be centred in its termini and not in the central, alanine-rich sequence (A113-G-AAAA-G-A120).

Keywords: Prion protein; TSE; BSE; Aggregation initiation; Aggregation propensity; Poly-proline II

1. Introduction

Transmissible spongiforme encephalopathies (TSEs) are a group of fatal neurodegenerative disorders leading to a large scale loss of neurons in the central nervous system. They affect man (CJD, FFI, GSS) and various animals (bovine spongiforme encephalopathy, scrapie, chronic wasting syndrome). According to the protein-only hypothesis [1], these diseases are caused by the conformational transition of the cellular prion protein, PrP^{C}, into the misfolded isoform PrP^{Sc}. Human PrP^{C} is a soluble cell surface glycoprotein of 231 residues, consisting of an unstructured amino-terminal domain and a mostly α-helical carboxy-terminal domain [2]. Its physiological function is not fully understood at the moment, but evidence points to an involvement in various cellular processes, such as regulation of presynaptic copper levels [3] and protection from oxidative stress [4], as well as several signal transduction pathways [5–7].

In contrast to the cellular prion protein, PrP^{Sc} is predominantly β-sheet, resistant to protease K, has a low solubility in non-denaturing solvents and aggregates readily into amyloid-like fibrils [1,8]. Recently, Wille et al. proposed a first structural model of PrP^{Sc} based on electron crystallography data with a resolution of about 7 Å [9,10]. According to this model, PrP^{Sc} adopts a β-helical structure, which incorporates the unstructured amino terminus as well as helix 1 and the short antiparallel β-sheet of PrP^{C}, while the disulfide-linked helices 2 and 3 retain their helical conformation.

Though the mechanism and initiation site of the prion conformational conversion is not known, it could be shown that only part of the PrP^{C} sequence is needed for the transconformation and the formation of amyloid fibrils [11]. Several short peptides derived from the amino-terminal region of the globular domain of PrP are known to aggregate in solution and exhibit cytotoxic properties. One major amyloidogenic sequence spanning residues 106–126 in human PrP contains the highly conserved, apolar AGAAAAGA palindrome [12]. In addition, amyloid formation could be observed for the sequences huPrP (106–147) [13], huPrP (118–135) [14], huPrP (132–160) and huPrP (124–167) [15]. All of these peptides fulfil one major criterion for amyloid formation, namely the adoption of unstructured or partially unstructured conformations [16].

Though amyloid formation may be a general property of polypeptides [17], the initiation of peptide aggregation is dependent on the presence of short sequence stretches which follow certain general rules [18], as well as on the absence of "gatekeeper" residues preventing β-sheet formation [19]. In particular, the presence of sequences composed of bulky, sterically restricted amino acid residues, which have been shown to display an intrinsic preference for extended, β-sheet like conformations in the random coil state by analysis of sequence corrected NMR chemical shifts [20], is supposed to enhance the fibril formation tendency of peptides. On the other hand, clusters of small amino acids, such as alanine or glycine, have backbone mobility much higher than an average random coil sequence [20]. Such clusters may be assumed to probe a large number of conformations in the Ramachandran plot on a very fast time scale minimizing the life time of individual, aggregation prone conformations.

As a consequence, even point mutations can dramatically alter the aggregation behaviour of proteins [21]. Because the pathogenic prion-conversion is likely to involve large-scale rearrangement of tertiary structure – as implied by the structures of PrP^{C} [2] and the model of Govaerts

*Corresponding author. Fax: + 49 921 553544.
E-mail address: stephan.schwarzinger@uni-bayreuth.de (S. Schwarzinger).

[1] These authors contributed equally to this work.

Abbreviations: PrP, prion protein; TSE, transmissible spongiforme encephalopathies; CJD, Creutzfeldt-Jakob disease; FFI, fatal familial insomnia; GSS, Gerstmann–Sträussler–Scheinker syndrome; EM, electron microscopy; CR, Congo Red; PPII, poly-proline II

0014-5793/$32.00
doi:10.1016/j.febslet.2006.03.002

et al. for PrP^{Sc} [9,10] – it is commonly accepted that at least partially unfolded intermediates are significantly populated during prion conversion. To obtain further insights into the mechanistic details of PrP^{Sc} formation, it is therefore of interest to investigate structural preferences in the random coil state of the corresponding sequence. Here, we perform a turbidimetric analysis of the aggregation behaviour of a series of overlapping peptides spanning residues 106–157 of human prion protein, which have been selected on the basis of pre-existing data on their conformational behaviour in the random coil state, to detect possible initiation sites for intermolecular aggregation. This sequence is largely identical to the interaction interface between heterologous forms of the prion protein, underscoring the importance to investigate in particular this sequence [22].

2. Materials and methods

2.1. Peptide design

Peptides for this study were selected to include different combinations of putative aggregation initiation sites, such as the apolar palindrome A113-GAAAAGA, β-sheet 1 (128–131), the sequence I138-IHF and the putative gatekeeper element helix 1 (144–154). Stabilizing (N153W) and destabilizing (R151G) mutants of PrP helix 1 were designed employing in-house written software [23]. To facilitate spectrophotometric determination of peptide concentrations, a tyrosine residue was added to the amino-terminus of peptides lacking tyrosine in their sequence.

2.2. Peptides

Peptides were purchased from Jerini AG (Berlin, Germany) and from Thermo Electron Corporation (Ulm, Germany) as HPLC-purified freeze dried powder containing trifluoroacetate counter ions. Peptides were protected by an amino-terminal acetyl group and by amidation at the carboxy-terminus to exclude charge effects from free termini. The sequences of the peptides under investigation are summarized in Fig. 1.

2.3. Aggregation tests

Buffer conditions applied here were optimized prior to this study with respect to lag-time and duration of transitions. Peptides were dissolved in 20 mM sodium acetate buffer containing 20% DMSO p.a. (Sigma–Aldrich, St. Louis, MO, USA) and 0.01% sodium azide to prevent bacterial growth (Fluka, Switzerland), pH 4.5, sonicated three times for 5 min each, centrifuged at 14 000 × g for 1 h, and stored as frozen stocks at −20 °C. After UV spectrophotometric determination of concentration using an ε_{mM} (280 nm) of 1.28 $mM^{-1}\,cm^{-1}$ (http://www.expasy.org/tools/protparam.html), all peptide samples were adjusted to a concentration of 50 μM, except for peptides encompassing helix 1. Initial absorptions in the samples were 0.0073 AU per residue with a standard deviation of 0.0026 AU. This small scatter – compared to the increases in absorbance measured in sigmoidal transitions upon aggregation – indicates the absence of aggregates at the beginning of measurements. Concentrations of helix 1 peptides were higher in order to be able to observe any transition (huPrP(140–158): 106 μM, huPrP(140–158)N153W: 94 μM; huPrP(140–158)R151G: 82 μM). Higher concentrations were not possible due to the limited solubility of selected peptides. To follow the time course of aggregation, the turbidity at 450 nm was measured every 3–6 h on an Uvikon 930 spectrophotometer (Kontron Instruments, Eching, Germany) for a total of 180 h in sealed 70 μl microcuvettes (Brand, Wertheim, Germany) to prevent volume- and concentration-changes due to solvent evaporation. Prior to each measurement samples were homogenized by careful agitation. Between measurements samples were stored at 23 °C. An identical cuvette filled with buffer without any peptide treated exactly as the samples was used a reference in turbidity measurements. Before each measurement, the photometer was zeroed using a cuvette with peptide free buffer solution.

2.4. Data evaluation

In order to obtain an estimate of the aggregation tendencies of the peptides, we have determined the approximate lag-time, the apparent rate of aggregation, and the midpoint of the aggregation transition. Lag-time was defined as the duration of approximately linear behaviour of the turbidimetric data and was determined by visual inspection. The approximate lag-time reported corresponds to the last data point prior to the aggregation transition. Assuming exponential growth data points past the lag-time were fit to an exponential growth function

$$A_{450} = A_{450}^{\text{lag-time}+1} + B(1 - e^{-kt})$$

where $A_{450}^{\text{lag-time}+1}$ represents the first data point past the approximate lag-time, B the parameter corresponding to the signal amplitude, and t the time in hours. k was taken as the apparent rate of aggregation. The midpoint of the aggregation transition, t_{aggr} was obtained by subtracting the approximate lag-time from the midpoint of the sigmoidal transition t_m. t_m was obtained by fitting the observed data to the sigmoid function

$$A_{450} = A_{450}^{t=0} + \frac{\Delta A_{450}}{1 + e^{-\frac{t-t_m}{b}}}$$

where ΔA_{450} represents the difference in turbidity between the initial and the final equilibrium state, giving a measure for the extent of aggregation, t denotes the time in hours, and b represents the width of the sigmoidal transition. Fitting was performed using the program SigmaPlot 2001 (SPSS Inc., Chicago, IL, USA).

2.5. Whole mount electron microscopy

Samples from turbidity assays were stored for additional three weeks at 4 °C to allow fibril formation to complete. For whole mount electron microscope (EM) samples were spun down at 18 000 × g for 1 h. Five microlitres from each tube were applied to a pioloform-coated copper grid (Plano GmbH, Marburg, Germany) and allowed to adhere for 10 min. The grids were stained with 1% aqueous uranyl acetate for 1–2 min. Samples were examined in a Zeiss 902A transmission electron microscope (Carl Zeiss, Oberkochen, Germany) operated at 80 kV. Micrographs were taken using SO-163 EM film (Kodak, Rochester, NY).

2.6. Congo Red (CR) staining

CR staining of fibril preparations was performed in a variation of Puchtler's method after turbidity measurements. Fibril containing samples were centrifuged at 10 000 × g for 30 min, the pellets were suspended to HistoBond slides and allowed to dry at 50 °C. The dried samples were stained with saturated CR solution in 80% ethanol containing 1 M NaCl for 20 min. Unbound CR was removed by washing in distilled water followed by rinsing with 80% ethanol. The stained and dried samples were subsequently embedded in *gummi arabicum* and visually inspected for birefringence under a polarization microscope (B1-220, MOTIC, Wetzlar, Germany) equipped with a SLR camera (Canon 350-D, Japan. *Note*. The colours seen are slightly distorted due to the inability to perform correct white balance with the camera mounted to the microscope; pictures were only γ-corrected to avoid further distortions of colour).

2.7. Calculation of aggregation propensities

Theoretical calculations of aggregation propensities of various peptide sequences and the influence of selected residues within these sequences have been carried out with the software TANGO (http://tango.embl.de) at a pH of 4.5 [24,25].

3. Results and discussion

The aim of this study was to determine possible or likely initiation regions of prion amyloid formation. Though there are several publications describing the aggregation behaviour of peptides encompassing the amino terminal region of the globular prion domain [12–15,26], the differences in conditions applied in theses studies make it difficult to assess relative

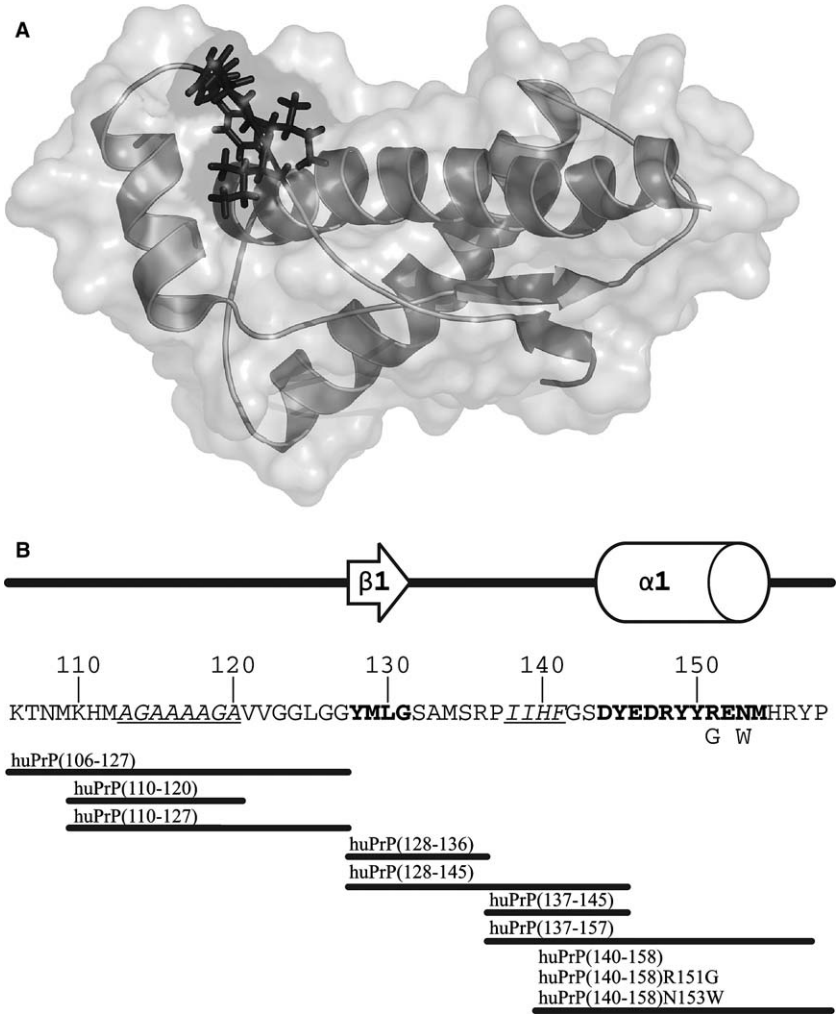

Fig. 1. (A) Structure of huPrP(121–231) [2]. The partially solvent exposed sequence of hydrophobic residues I138-IHF is shown as dark gray sticks. (B) Schematic overview over the amino acid sequence of huPrP(106–158) and the peptides used in this study . The secondary structure representation shows structural elements derived from the NMR structure [2]. Putative aggregation sites are printed italic underlined, the putative gatekeeper element α-helix 1 and β-strand 1 are printed bold. The positions of the designed stabilizing (N153W) and destabilizing (R151G) mutations are also indicated [23].

aggregation tendencies. Therefore, to obtain a comparable data set for the whole 106–157 region we performed turbidimetric aggregation assays on a series of overlapping peptides corresponding to this sequence. Turbidimetry is a rapidly available assay for the qualitative description of an aggregation process, which does not allow the determination of the aggregates size such as light scattering methods do. The application of the latter, however, is limited in the case of small peptides at very low concentrations. The peptides were chosen to encompass all structural elements present in this region, as well as all known functionally important sequences, like the cytotoxic palindrome and the regions important for the species barrier. A set of peptides with comparable lengths (huPrP(110–120), huPrP(128–136), huPrP(137–145)) was chosen to allow easy comparison of aggregation parameters for the different structural and functional elements. Additional peptides were introduced into the study to allow the investigation of effects of flanking sequences (see Fig. 1).

All investigated peptides adopt a random coil conformation in their soluble monomeric state, with the exception of the 145–155 region (helix 1 in the structure of the full length prion protein), which shows a tendency to populate helical conformations in isolated peptides [27]. The key parameters of the measured peptide aggregation are summarized in Table 1 (apparent aggregation rate k, t_m, t_{aggr}, lag-time, ΔA_{450}). In repeated measurements of several samples which were prepared under apparently identical conditions, outliers with a markedly faster aggregation could be observed in several series. However, the majority of measurements showed consistent experimental values. A similar phenomenon has been reported in a recent study by Hortschansky et al., who investigated several derivatives of the Aβ peptides and found large deviations of transition midpoints and rates for apparently identical samples [28]. In this report the amount of scatter as well as the lag-time correlate with the peptide concentration: less peptide results in larger scatter and longer lag-times. The authors conclude that even under strongly controlled experimental conditions, peptide polymerization reactions are highly influenced by stochastic factors. In the present study, the peptide concentration could not be further increased. However, the relative aggregation tendencies reported could be reproduced in independent measurements (data not shown).

3.1. The sequence immediately preceding helix 1 has a higher aggregation propensity than β-strand 1 (see Table 1)

huPrP(128–136), which includes β-strand 1 and which was used here as paradigmatic model for β-strand self-association, showed a clear transition with a t_{aggr} of 28 h and an average apparent rate k of 0.024 h^{-1}. The difference in absorbance was between 0.1 and 0.15 AU. Such a clear transition was expected as single β-strands have a well-known tendency for self-association. huPrP(137–145), which corresponds to the loop between β-strand 1 and helix 1, displayed a much faster course of aggregation with a t_{aggr} of approximately 7–8 h and an apparent rate k of 0.15 h^{-1} and a slightly reduced approximate lag-time. Both peptides are of the same length, and each of them contains one possible initiation site for aggregate formation: β-strand 1, which is part of the huPrP(128–136) peptide, has been implicated in fibril formation in studies on the peptide huPrP(118–135). huPrP(137–145) contains a region of bulky apolar residues immediately preceding helix 1 (I138-IHF), which showed a tendency to adopt extended conformations in NMR studies of peptides containing the helix 1 region of huPrP [27]. While huPrP(128–135) shows fine fibrillar aggregates, the aggregates of huPrP(137–145) appear to be highly ordered, in a nearly crystalline structure (see Fig. 2).

Despite being experimentally identified as a putative aggregation association site, this sequence is not detected by TANGO algorithm, which predicts aggregation propensities. This apparently is due to the positive charge of the His residue at the pH of 4.5. At higher pH, when histidine is uncharged, a small aggregation propensity is detected by the TANGO algorithm. Exchange of Tyr, which has similar steric requirements, for His, however, results in a high calculated aggregation propensity (see Table 2A). Therefore, a comparison of several species specific polymorphism contained in this region with TANGO was performed on the IIYF background. Interestingly, I138-I (human) and L138-I (bovine and ovine) exhibited a comparable aggregation score in TANGO, while M138-I (mouse) and M138-M (syrian hamster) showed a significant decrease in the calculated aggregation propensity, with M138-M being the least aggregation prone sequence (see Table 2B). This might at least partially account for the difficulty of experimental TSE transmission from bovine and human sources to hamsters and mice. The exposed structural position of the IIHF-sequence further stresses its possible importance in the aggregation initiation and interaction between PrP^{C} and PrP^{Sc} (see Fig. 1). In fact, a recent study by Vanik et al., who used peptides corresponding to the sequences 23–144 of man, mouse, and hamster, revealed the same order of aggregation susceptibility as suggested by TANGO. Also, cross seeding experiments could demonstrate the importance of this sequence for the species barrier [29]. Further, the IIHF-sequence was identified as contact site between different prion proteins as an early step in the transconformation process in a

Table 1
Overview of aggregation parameters obtained from fitting the measured turbidity curves to a sigmoid function

Peptide	k, apparent rate of aggregation	Approximate lag-time (h)	t_m (h)	t_{aggr} (h) (lag-time – t_m)	ΔA_{450}
huPrP(110–127)B[a]	0.055 ± 0.017	48	64 ± 2	16	0.029
huPrP(128–136)A	0.036 ± 0.003	12	31 ± 2	19	0.127
huPrP(128–136)B	0.023 ± 0.003	16	48 ± 1	32	0.105
huPrP(128–136)C	0.012 ± 0.003	12	46 ± 11	34	0.175
Average	0.0237	13.3	41.7	28.3	–
huPrP(128–145)A[b]	n.a.	16	18–21	1–2	0.050
huPrP(128–145)B	(0.32 ± 0.06)	16	(52 ± 7)	(36)	0.027
huPrP(128–145)C[b]	n.a.	16	18–21	1–2	0.012
Average	n.a.	16	18–21	1–2	–
huPrP(137–145)A[c]	n.a.	n.a.	n.a.	n.a.	0.004
huPrP(137–145)B	0.16 ± 0.03	8	15 ± 2	7	0.019
huPrP(137–145)C	0.14 ± 0.02	8	16 ± 2	8	0.017
Average	0.15	8	15.5	7.5	–
huPrP(137–157)A[d]	n.a.	0	n.a.	n.a.	n.a.
huPrP(137–157)B	0.026 ± 0.004	36	65 ± 2	33	0.045
huPrP(137–157)C	0.018 ± 0.002	28	66 ± 2	38	0.087
Average	0.022	32	65.5	35.5	–
huPrP(140–158)R151G[e]	0.06 ± 0.02	101	131 ± 15	30	0.034

k is the apparent rate of aggregation, t_m is the calculated mid-point of the experimental data fitted to a sigmoidal transition. The lag-time column indicates the time before onset of the transition. t_{aggr} is t_m subtracted from the lag-time measuring the speed of the aggregation reaction. ΔA_{450} shows the difference between initial state and after the transition. Except for helix 1-peptides, three apparently identical samples have been prepared (A, B, and C) for each peptide, which have been independently measured. Peptides not shown in this table exhibited no measurable aggregation in the turbidimetric assay (huPrP(106–127); huPrP(110–127)A and C; huPrP(110–120); huPrP(140–158) wt and N153W).

[a]huPrP(110–127)B was the only sample including the alanine-rich sequence (out of nine) that showed a transition under the experimental conditions applied in this study.

[b]No fit was possible due to extremely fast aggregation of huPrP(128–136)A and C within two data points. In this case, t_m and t_{aggr} were approximately determined by estimation. The average was calculated from these two data sets.

[c]Denotes entries for which no fit was possible due to low of aggregation as indicated by the small ΔA_{450}.

[d]No fit was possible for huPrP(137–158) due to a non-sigmoidal behaviour of the data.

[e]Aggregation was only observed for the destabilized variant R151G of the peptide corresponding to helix 1.

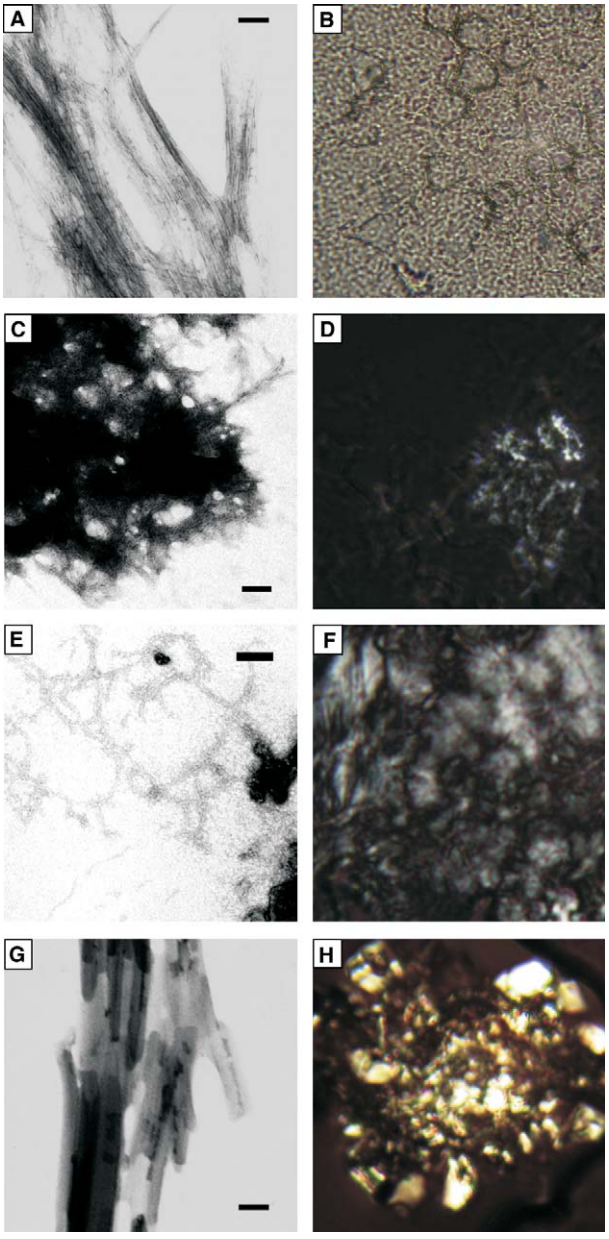

Fig. 2. Electron micrographs (left column) and CR stains (right column) for selected peptides are shown on page 5. The black bar in the EM pictures corresponds to 100 nm. (A) EM, huPrP(106–127); (B) CR stain, huPrP(106–127); (C) EM, huPrP(110–127); (D) CR stain, huPrP(110–127); (E) EM, huPrP(128–136); (F) CR stain, huPrP(128–136); (G) EM, huPrP(137–145); (H) CR stain, huPrP(137–145). Although peptides huPrP(106–127) and huPrP(110–127), which contain the alanine-rich palindrome, did not produce observable transitions in the turbidimetric assay, aggregates were formed during prolonged incubation (panels A and C) – in contrast to huPrP(1110–120), which never formed aggregates. Panel E, showing huPrP(128–136), which includes the sequence of β-strand 1 that has been used as model for the aggregation of an isolated β-structure, exhibits only very thin fibrillar aggregates. huPrP(137–145), including the IIHF-motive, apparently forms highly ordered aggregates (panel G), which, however, display the typical golden-green birefringence expected for amyloidogenic aggregates in CR stains (panel H).

recent molecular dynamics study published by DeMarco and Daggett [30]. As pointed out earlier, the structural conversion of PrP^{C} to PrP^{Sc} likely involves an order-to-disorder-to-order transition of the sequence prior to helix 2. In view of recent result it appears likely that aggregation actually starts from partially disordered states [31,32], which are present even under equilibrium conditions [33–35]. It has been shown that sequences with neighbouring large, hydrophobic amino acids favour extended, β-like conformations even under strongly denaturing conditions [20]. Thus, even in the disordered state, I138-IHF is likely to populated sheet-like conformations due to intrinsic amino acid properties. Indeed, such a conformational preference could be detected in peptide models [27]. Therefore, I138-IHF can serve as an aggregation site either for homo- or for hetero-sequence aggregation, e.g., with the alanine-rich sequence [30].

3.2. Helix 1 has no tendency to form aggregates, it can delay but not prevent fibril formation in longer peptides

Further sigmoidal transitions could be observed for peptides huPrP(128–145), huPrP(137–145) and huPrP(137–157), although the differences in absorbance were less pronounced, which may be related to differences in morphology and size between peptide aggregates. In contrast to the abovementioned peptides, peptides consisting solely of helix 1 (huPrP(140–158) and its stabilized variant N153W), excluding the flanking sequences, showed no aggregation tendency whatsoever. Only a destabilized variant, huPrP(140–158)-R151G, showed a very slow, shallow transition which could be observed after 101 h (see Table 1). Here, the intense network of salt-bridges and favourable electrostatic interactions within helix 1 is distorted, obviously enabling aggregation, presumably by interaction of aromatic residues.

However, adding the sequence of helix 1 to strongly aggregating peptides like huPrP(128–145) did not abolish fibril formation, but nevertheless delayed the formation of aggregates to an average lag-time of 30 h for huPrP(137–157), compared to 8 h for huPrP(137–145), and 16 h for huPrP(128–145), which is approximately of the same length. The growth phase of aggregates measured by t_{aggr}, however, is much longer (see Table 1).

This leads to the possibility that helix 1 might remain in a helical conformation during the early stages of the transconformation process. This is again supported by the study of molecular dynamics data recently published by DeMarco and Daggett, which showed no conversion of helix 1 during the simulated protofibril formation [30]. Later in the course of the conformational transition, facilitated by conformational changes in its surroundings, the energetically unfavourable conversion of helix 1 into an extended structure could take place. This is in line with studies showing the existence of helical PrP dimers in the early stages of the SDS induced prion transconformation, which later form higher oligomers rich in β-sheet elements [36]. As previously hypothesized [27], helix 1 might play the role of a ''gatekeeper'' element in the aggregation process, by acting as an energetic barrier for the transconformation of PrP.

3.3. The alanine-rich sequence requires flanking parts of the sequence to form fibrillar aggregates

The palindromic alanine-rich sequence A113-GAAAGA is believed to be causal for neuro-inflammation induced by the peptide PrP(106–126). Interestingly, huPrP(106–126) did not show an observable transition that would indicate aggregate

Table 2
Summary of TANGO calculations

A *S132-AMSRP-IIHF-GSDY-E146*

Wt–pH 4.5	Wt–pH 8.5	P137V	H140A	H140Y
0.0%	0.5%	0.9%	17.3%	47.8%

B *S132-AMSRP-[II][LI][MI][MM]-YFGSDY-E146*

–IIHF– (human)	–LIHF– (bovine/sheep)	–MIHF– (mouse)	–MMHF– (hamster)
47.8%	31.4%	8.8%	0.9%

C *A113-AGAAAAGAVVGGLGGYML-G131*

	Wt	A117V	G119A	M129V
A113 → G131	1.1%	9.4%	7.1%	2.5%
A113 → A120-	0.9%	10.6%	7.3%	0.9%
-V121–V122-	2.2%	17.2%	13.5%	4.0%
-G123 → G131	0.2%	0.5%	0.5%	2.6 %

A – Aggregation propensity of the IIHF-region: influence of the charge pattern on aggregation propensities. B – Effects of species specific sequence variations: I138 and I139 vary considerably among species and have a strong effect on the aggregation propensity (*Note*. Variant H140Y has been used to estimate species specific effects; see panel A). C – Influence of single residue substitutions on the aggregation propensities of the sequence huPrP(113–131) and selected sub-sequences (huPrP(A113–A120), huPrP(V121–V122), and huPrP(G123–G131), which includes β-strand 1). It shall

formation within 180 h under our conditions.[2] The same holds true for huPrP(110–120), which contains almost exclusively the alanine-rich region, and for huPrP(120–127), which contains additional hydrophobic residues. Prolonged incubation of huPrp(106–127) and huPrP(110–127) finally leads to aggregate formation. The aggregates of huPrP(106–127) exhibit a typical fibrillar morphology in the ER, almost resembling a disordered arrangement of protofibrils, whereas huPrP(110–127) forms amorphous aggregates (see Fig. 2). Regardless of the morphology, in both cases the aggregates showed the typical red-green birefringence in a CR stain, indicating the presence of amyloid (see Fig. 2). However, it was not possible to perform CR-staining nor to detect aggregates in EM-micrographs for huPrP(110–120).

These results are somewhat surprising, as several other studies implicated the apolar palindromic sequence AGAAAAGA in fibril formation and cytotoxicity of peptides around the 110–120 region [12,37,38]. Nevertheless, our data do not contradict the importance of the palindromic sequence for the conformational transition of PrP. Molecular dynamics studies showed the importance of a template for the re-folding of this sequence [30], whereas our studies only tested for auto-aggregation within the same sequence. In particular, protofibril models derived from such simulations showed a β-core made up from residues 116–119, adding as a third strand to the native β-sheet, the elongated native sheet itself and another strand containing residues 135–140, underlining the importance of I138-IHF for the pathogenic process. Importantly, inter-prion contacts in this model are formed between residues 116–119 (alanine-rich) and residues 135–140, corresponding to the above proposed IIH(F) aggregation site.

Extending the 110–126 peptide on the amino terminal side to form huPrP(106–126), however, restores the alanine-rich peptide's (huPrP(110–120)) ability to form amyloid-like fibrillar plaques (see Fig. 2). This points to a role of the 106–110 region as another possible initiator site, which is further underscored by the importance of the 90–112 region for prion infectivity [39]. So, while the palindromic region might not be able to form amyloid fibrils by itself, it may be included into fibrillar structures, whose formation is initiated by other regions of the peptide. Further evidence for this behaviour could be found in TANGO calculations of aggregation propensities (see Table 2C). The isolated AGAAAAGA showed a low TANGO score due to the presence of flexibility increasing Gly residues [20], which have also been shown to be evolutionary conserved in order to prevent aggregation in other cases [40]. However, elongation of the sequence to AGAAAAGAVV, as well as the introduction of the pathogenic A117V mutation [41] increased the calculated aggregation tendency of the peptide indicating that the aggregation propensity is introduced by the valine residues. An explanation for this behaviour can be found in the conformational propensity of the palindromic region. Conformationally flexible, short Ala-rich peptides are known to preferentially populate polyproline type II-like conformations, which are close to extended conformers in the Ramachandran space [42]. The presence of rather bulky Val residues, however, might shift the conformational distribution in the direction of β-sheets [43]. The propensity for poly-proline II (PPII) like conformations also offers an explanation for the need for a template in the aggregation process, as PPII helices show an intrinsic tendency to interact and form coiled-coils, such as in collagen. Proline rich peptides, such as iPrP13 (DAPAAPAGPAVPV), which has been designed to inhibit aggregation into β-sheets [44], could therefore present an ideal template. Indeed Soto et al. could show that iPrP13 interacts with the AGAAAAGA palindrome and interferes with the prion transconformation – possibly by presenting a stronger interacting template for the palindrome than natural interaction partners like I138-IHF. Further experimental evidence can be deduced from the work of Chabry et al., who found that peptides encompassing the palindromic region (113–141, 115–141, 117–141 and 119–141) could inhibit the conversion of full length prion protein in a dosis-dependent manner, while the only marginally shorter peptide 121–141 showed no inhibitory effect [45].

[2] NB: Transitions of alanine-rich peptides could be observed within the observation periode at higher concentrations in this study as well as under other experimental conditions in other studies.

In summary, our study results in two major findings, namely that the bulky, apolar, and highly surface-exposed I138-IHF sequence is a possible initiation site for aggregation and that the aggregation properties of the neurotoxic peptide huPrP(106–126) are centred at residues 106–110 and VV(121–122), respectively. Recent molecular dynamics simulations of the PrP^{C} to PrP^{Sc} conversion [30] as well as studies concerning the species barrier [29] also point to the importance of those regions in the aggregation initiation process. The crucial role of these structural elements is further underscored by the existence of several pathogenic mutations. Our TANGO calculations indicate that the important M129V polymorphism, which is located in β-strand 1 and is responsible for phenotypic heterogeneity of prion diseases [46] and susceptibility for the classical and new variant Creutzfeldt-Jakob Disease (CJD) [47], changes the aggregation propensity in the VV(121–122) region. In addition, the Gerstmann–Sträussler–Scheinker syndrome (GSS)-causing G131V mutation, also located in β-strand 1, could be shown to increase local conformational plasticity, thereby facilitating prion transconformation [47]. Thus, if β-strand 1 becomes exposed during structural rearrangements, it may also efficiently enhance aggregation as shown here. The only amyloidogenic element described here which does not harbor any pathogenic mutations is the I138-IHF sequence. However, the differences in sequence between various species suggest a role of this region in the species barrier. We have shown that IIHF has the ability to aggregate fast compared to, e.g., β-strand 1. With β-strand 1 being hidden in PrP^{C}, this makes the partially surface-exposed I138-IHF motive the most important identified aggregation promoting element in PrP. In combination with recent data from the literature a concerted operation of several amyloidogenic elements appears a likely mechanism in formation of inter-prion protein contacts. Interaction of different elements may also explain the conformational heterogeneity observed in prion strains.

Acknowledgements: We are grateful to Dr. M. Fändrich for helpful discussions on methodology and aggregation of peptides in general in the initial phase of the project. This work was supported by grants from the State of Bavaria (FORPRION) and the VW-foundation (I-79 968). A figure containing the turbidimetric data is available as supplementary material.

Appendix A. Supplementary data

Supplementary data associated with this article can be found, in the online version, at doi:10.1016/j.febslet.2006.03.002.

References

[1] Prusiner, S.B. (1998) Prions. Proc. Natl. Acad. Sci. USA 95, 13363–13383.
[2] Zahn, R., Liu, A., Luhrs, T., Riek, R., von, S.C., Lopez, G.F., Billeter, M., Calzolai, L., Wider, G. and Wuthrich, K. (2000) NMR solution structure of the human prion protein. Proc. Natl. Acad. Sci. USA 97, 145–150.
[3] Brown, D.R. (2001) Copper and prion disease. Brain Res. Bull. 55, 165–173.
[4] Martins, V.R. and Brentani, R.R. (2002) The biology of the cellular prion protein. Neurochem. Int. 41, 353–355.
[5] Chiarini, L.B., Freitas, A.R., Zanata, S.M., Brentani, R.R., Martins, V.R. and Linden, R. (2002) Cellular prion protein transduces neuroprotective signals. EMBO J. 21, 3317–3326.
[6] Mouillet-Richard, S., Ermonval, M., Chebassier, C., Laplanche, J.L., Lehmann, S., Launay, J.M. and Kellermann, O. (2000) Signal transduction through prion protein. Science 289, 1925–1928.
[7] Zanata, S.M., Lopes, M.H., Mercadante, A.F., Hajj, G.N., Chiarini, L.B., Nomizo, R., Freitas, A.R., Cabral, A.L., Lee, K.S., Juliano, M.A., de Oliveira, E., Jachieri, S.G., Burlingame, A., Huang, L., Linden, R., Brentani, R.R. and Martins, V.R. (2002) Stress-inducible protein 1 is a cell surface ligand for cellular prion that triggers neuroprotection. EMBO J. 21, 3307–3316.
[8] Pan, K.M., Baldwin, M., Nguyen, J., Gasset, M., Serban, A., Groth, D., Mehlhorn, I., Huang, Z., Fletterick, R.J. and Cohen, F.E., et al. (1993) Conversion of alpha-helices into beta-sheets features in the formation of the scrapie prion proteins. Proc. Natl. Acad. Sci. USA 90, 10962–10966.
[9] Govaerts, C., Wille, H., Prusiner, S.B. and Cohen, F.E. (2004) Evidence for assembly of prions with left-handed beta-helices into trimers. Proc. Natl. Acad. Sci. USA 101, 8342–8347.
[10] Wille, H., Michelitsch, M.D., Guenebaut, V., Supattapone, S., Serban, A., Cohen, F.E., Agard, D.A. and Prusiner, S.B. (2002) Structural studies of the scrapie prion protein by electron crystallography. Proc. Natl. Acad. Sci. USA 99, 3563–3568.
[11] Kundu, B., Maiti, N.R., Jones, E.M., Surewicz, K.A., Vanik, D.L. and Surewicz, W.K. (2003) Nucleation-dependent conformational conversion of the Y145 Stop variant of human prion protein: structural clues for prion propagation. Proc. Natl. Acad. Sci. USA 100, 12069–12074.
[12] De Gioia, L., Selvaggini, C., Ghibaudi, E., Diomede, L., Bugiani, O., Forloni, G., Tagliavini, F. and Salmona, M. (1994) Conformational polymorphism of the amyloidogenic and neurotoxic peptide homologous to residues 106–126 of the prion protein. J. Biol. Chem. 269, 7859–7862.
[13] Tagliavini, F., Prelli, F., Verga, L., Giaccone, G., Sarma, R., Gorevic, P., Ghetti, B., Passerini, F., Ghibaudi, E. and Forloni, G., et al. (1993) Synthetic peptides homologous to prion protein residues 106–147 form amyloid-like fibrils in vitro. Proc. Natl. Acad. Sci. USA 90, 9678–9682.
[14] Pillot, T., Lins, L., Goethals, M., Vanloo, B., Baert, J., Vandekerckhove, J., Rosseneu, M. and Brasseur, R. (1997) The 118–135 peptide of the human prion protein forms amyloid fibrils and induces liposome fusion. J. Mol. Biol. 274, 381–393.
[15] Jamin, N., Coic, Y.M., Landon, C., Ovtracht, L., Baleux, F., Neumann, J.M. and Sanson, A. (2002) Most of the structural elements of the globular domain of murine prion protein form fibrils with predominant beta-sheet structure. FEBS Lett. 529, 256–260.
[16] Dobson, C.M. (1999) Protein misfolding, evolution and disease. Trends Biochem. Sci. 24, 329–332.
[17] Chiti, F., Webster, P., Taddei, N., Clark, A., Stefani, M., Ramponi, G. and Dobson, C.M. (1999) Designing conditions for in vitro formation of amyloid protofilaments and fibrils. Proc. Natl. Acad. Sci. USA 96, 3590–3594.
[18] Lopez de la, P.M. and Serrano, L. (2004) Sequence determinants of amyloid fibril formation. Proc. Natl. Acad. Sci. USA 101, 87–92.
[19] Thirumalai, D., Klimov, D.K. and Dima, R.I. (2003) Emerging ideas on the molecular basis of protein and peptide aggregation. Curr. Opin. Struct. Biol. 13, 146–159.
[20] Schwarzinger, S., Dyson, H.J. and Wright, P.E. (2002) Molecular hinges in protein folding: the urea-denatured state of apomyoglobin. Biochemistry 41, 12681–12686.
[21] Ventura, S. and Serrano, L. (2004) Designing proteins from the inside out. Proteins 56, 1–10.
[22] Horiuchi, M., Priola, S.A. and Caughy, B. (2000) Interactions between heterologous forms of prion protein: binding, inhibition of conversion, and species barriers. Proc. Natl. Acad. Sci. USA 97, 5836–6841.
[23] Ziegler, J. and Schwarzinger, S. Genetic algorithms as a tool for helix design – computational and experimental studies on prion protein helix 1, J. Comp. Aided Mol. Design (in press).
[24] Fernandez-Escamilla, A.M., Rousseau, F., Schymkowitz, J. and Serrano, L. (2004) Prediction of sequence-dependent and mutational effects on the aggregation of peptides and proteins. Nat. Biotechnol. 22, 1302–1306.

[25] Linding, R., Schymkowitz, J., Rousseau, F., Diella, F. and Serrano, L. (2004) A comparative study of the relationship between protein structure and beta-aggregation in globular and intrinsically disordered proteins. J. Mol. Biol. 342, 345–353.
[26] Zahn, R. (2003) The octapeptide repeats in mammalian prion protein constitute a pH-dependent folding and aggregation site. J. Mol. Biol. 334, 477–488.
[27] Ziegler, J., Sticht, H., Marx, U.C., Muller, W., Rosch, P. and Schwarzinger, S. (2003) CD and NMR studies of prion protein (PrP) helix 1 – novel implications for its role in the PrPC → PrPSc conversion process. J. Biol. Chem. 278, 50175–50181.
[28] Hortschansky, P., Schroeckh, V., Christopeit, T., Zandomeneghi, G. and Fandrich, M. (2005) The aggregation kinetics of Alzheimer's beta-amyloid peptide is controlled by stochastic nucleation. Protein Sci. 14, 1753–1759.
[29] Vanik, D.L., Surewicz, K.A. and Surewicz, W.K. (2004) Molecular basis of barriers for interspecies transmissibility of mammalian prions. Mol. Cell 14, 139–145.
[30] DeMarco, M.L. and Daggett, V. (2004) From conversion to aggregation: protofibril formation of the prion protein. Proc. Natl. Acad. Sci. USA 101, 2293–2298.
[31] Legname, G., Baskakov, I.V., Nguyen, H.O., Riesner, D., Cohen, F.E., DeArmond, S.J. and Prusiner, S.B. (2004) Synthetic mammalian prions. Science 305, 673–676.
[32] Bocharova, O.V., Breydo, L., Parfenov, A.S., Salnikov, V.V. and Baskakov, I.V. (2005) In vitro conversion of full-length mammalian prion protein produces amyloid form with physical properties of PrP(Sc). J. Mol. Biol. 346, 645–659.
[33] Kuwata, K., Li, H., Yamada, H., Legname, G., Prusiner, S.B., Akasaka, K. and James, T.L. (2002) Locally disordered conformer of the hamster prion protein: a crucial intermediate to PrP^{Sc}? Biochemistry 41, 12277–12283.
[34] Hosszu, L.L.P., Wells, M.A., Jackson, G.S., Jones, S., Batchelor, M., Clarke, A.R., Craven, C.J., Waltho, J.P. and Collinge, J. (2005) Definable equilibrium states in the folding of human prion protein. Biochemistry 44, 16649–16657.
[35] Apetri, A.C., Surewicz, K. and Surewicz, W.K. (2004) The effect of disease-associated mutations on the folding pathway of human prion protein. J. Biol. Chem. 279, 18008–18014.
[36] Jansen, K., Schafer, O., Birkmann, E., Post, K., Serban, H., Prusiner, S.B. and Riesner, D. (2001) Structural intermediates in the putative pathway from the cellular prion protein to the pathogenic form. Biol. Chem. 382, 683–691.
[37] Gasset, M., Baldwin, M.A., Lloyd, D.H., Gabriel, J.M., Holtzman, D.M., Cohen, F., Fletterick, R. and Prusiner, S.B. (1992) Predicted alpha-helical regions of the prion protein when synthesized as peptides form amyloid. Proc. Natl. Acad. Sci. USA 89, 10940–10944.
[38] Kurganov, B., Doh, M. and Arispe, N. (2004) Aggregation of liposomes induced by the toxic peptides Alzheimer's Abetas, human amylin and prion (106–126): facilitation by membrane-bound GM1 ganglioside. Peptides 25, 217–232.
[39] Moroncini, G., Kanu, N., Solforosi, L., Abalos, G., Telling, G.C., Head, M., Ironside, J., Brockes, J.P., Burton, D.R. and Williamson, R.A. (2004) Motif-grafted antibodies containing the replicative interface of cellular PrP are specific for PrPSc. Proc. Natl. Acad. Sci. USA 101, 10404–10409.
[40] Parrini, C., Taddei, N., Ramazotti, M., Degl'Innocenti, D., Dobson, C.M. and Chiti, F. (2005) Glycine residues appear to be evolutionary conserved for their ability to inhibit aggregation. Structure 13, 1143–1151.
[41] Hedge, R.S., Mastrianni, J.A., Scott, M.R., DeFea, K.A., Tremblay, P., Torchia, M., DeArmond, S.J., Prusiner, S.B. and Lingappa, V.R. (1998) A transmembrane form of the prion protein in neurodegenerative disease. Science 279, 827–834.
[42] Shi, Z., Olson, C.A., Rose, G.D., Baldwin, R.L. and Kallenbach, N.R. (2002) Polyproline II structure in a sequence of seven alanine residues. Proc. Natl. Acad. Sci. USA 99, 9190–9195.
[43] Chen, K., Liu, Z., Zhou, C., Shi, Z. and Kallenbach, N.R. (2005) Neighbor effect on PPII conformation in alanine peptides. J. Am. Chem. Soc. 127, 10146–10147.
[44] Soto, C., Kascsak, R.J., Saborio, G.P., Aucouturier, P., Wisniewski, T., Prelli, F., Kascsak, R., Mendez, E., Harris, D.A., Ironside, J., Tagliavini, F., Carp, R.I. and Frangione, B. (2000) Reversion of prion protein conformational changes by synthetic beta-sheet breaker peptides. Lancet 355, 192–197.
[45] Chabry, J., Caughy, B. and Chesebro, B. (1998) Specific inhibition of in vitro formation of protease-resistant prion protein by synthetic peptides. J. Biol. Chem. 273, 13203–13207.
[46] Goldfarb, L.G., Petersen, R.B., Tabaton, M., Brown, P., LeBlanc, A.C., Montagna, P., Cortelli, P., Julien, J., Vital, C. and Pendelbury, W.W., et al. (1992) Fatal familial insomnia and familial Creutzfeldt-Jakob disease: disease phenotype determined by a DNA polymorphism. Science 258, 806–808.
[47] Jackson, G.S. and Collinge, J. (2001) The molecular pathology of CJD: old and new variants. Mol. Pathol. 54, 393–399.